

SnTUD-1: a solid acid catalyst for three component coupling reactions at room temperature†

Cite this: DOI: 10.1039/c3gc40792f

Muthusamy Poomalai Pachamuthu,^a Kannan Shanthi,^a Rafael Luque*^b and Anand Ramanathan*^c

A novel wormhole structured mesoporous material containing tin, SnTUD-1, was prepared by a direct hydrothermal synthesis method using triethanolamine (TEA) as an organic inexpensive mesoporous structure directing agent. XRD and N₂ sorption studies of SnTUD-1 confirmed the amorphous mesoporous nature of SnTUD-1, which possessed a large surface area of 555 m² g⁻¹ and a pore diameter of 7.4 nm. HR-TEM further ascertained the disordered pores in their morphology and the presence of nano-domains of SnO₂ species. The nature of the Sn⁴⁺ ion co-ordination with the silica matrix was evaluated by using different techniques including diffuse reflectance UV-Vis, FTIR, ²⁹Si MAS NMR and XPS. SnTUD-1 had an interesting Lewis acidity as measured by FTIR of pyridine adsorption which provided excellent activities in one-pot three-component Mannich-type reactions of ketones with aldehydes and amines at room temperature.

Received 26th April 2013,

Accepted 18th June 2013

DOI: 10.1039/c3gc40792f

www.rsc.org/greenchem

1. Introduction

Heterogeneous solid acid catalysts have been increasingly investigated in recent years due to their important applications in greener organic synthesis and more environmentally sound catalytic processes in replacement of mineral homogeneous acids.^{1,2} Ordered porous silicates constitute a relevant family of materials which have found extensive applications as catalyst supports, separation, adsorption *etc.* due to their large surface area and uniform pore sizes.³ Pure siliceous silicates have been conveniently modified in various ways (*e.g.* incorporation of Al³⁺, Fe³⁺, Ga³⁺, Zr⁴⁺, Sn⁴⁺ either during the synthetic procedure or post-synthesis) to develop acidity rendering catalytically active materials in acid-catalysed processes. Tin based silicates have been utilized as Lewis acid catalysts in a range of important organic transformations,^{4–10} with tin containing mesoporous molecular sieves employed in the conversion of bulkier substrates. Particularly, tin based mesoporous materials Sn-MCM-41,^{11–14} Sn-MCM-48,¹⁵ Sn-SBA-15,^{16–19} Sn-HMS,^{20,21} and Sn-PMO²² have been utilised in recent years as

redox and solid acid catalysts for a number of industrially relevant chemistries.

Among the mesoporous silicate family, a variety of catalytically active TUD-1 type materials have been reported in recent years following the original report of the purely siliceous TUD-1.²³ TUD-1 preparation featured a simple, low cost templating (TEA) synthesis route which was able to produce materials with three dimensional interconnected pores, tunable pore sizes and the possibility of higher incorporation of active metal ions (M⁺).²⁴ In view of the recent interests of the groups in terms of the design of novel highly active nanoporous materials for catalytic applications, we have been interested in exploring Sn incorporation into TUD-1 to develop SnTUD-1 materials with catalytic applications in multicomponent reactions. These chemistries have been carried out using homogeneous as well as heterogeneous catalyst systems.^{25,26} One type of such important multicomponent chemistries are Mannich type reactions, as β-amino carbonyl compounds are some of the most essential intermediates for the construction of various nitrogen containing natural products and pharmaceuticals.^{27–29} For this type of C–C bond forming reaction, different types of acid catalysts have been reported, including bismuth triflate,³⁰ WO_x–ZrO₂,³¹ NbCl₅,³² HClO₄–SiO₂,³³ adenine (aminocatalyst),³⁴ quaternary ammonium salt (QAS) Gemini fluorosurfactants,³⁵ Nafion-H®,³⁶ SiO₂–AlCl₃,³⁷ heteropoly acids,³⁸ indium trichloride,³⁹ Cu-nanoparticles⁴⁰ and inorganic–organic hybrid silica based tin(II) catalyst.⁴¹

Herein, we report for the first time the direct incorporation of Sn⁴⁺ into TUD-1 material that produced a catalytically active

^aDepartment of Chemistry, Anna University, Chennai, 600025, India^bDepartamento de Química Organica, Universidad de Cordoba, Campus de Rabanales, Edificio Marie Curie (C-3), Ctra Nnal IV-A, Km 396, 14014 Cordoba, Spain. E-mail: q62alsor@uco.es; Fax: +34 212066; Tel: +34 957211050^cCenter for Environmentally Beneficial Catalysis, The University of Kansas, Lawrence, KS 66047, USA. E-mail: anand@ku.edu; Fax: +1-785-864-6051;

Tel: +1-785-864-1631

†Electronic supplementary information (ESI) available. See DOI: 10.1039/c3gc40792f

SnTUD-1 in Mannich-type three component coupling reactions at room temperature.

2. Experimental

2.1. Synthesis of SnTUD-1

Tin containing mesoporous TUD-1 with a Si/Sn molar ratio of 50 was synthesized by a sol-gel method followed by hydrothermal treatment based on our previously reported procedure.⁴² SnTUD-1(50) was synthesized using tetraethyl-orthosilicate (TEOS, Sigma Aldrich, 99%) and tin tetrachloride ($\text{SnCl}_4 \cdot 5\text{H}_2\text{O}$, Sigma Aldrich, 98%) as silicon and tin precursors, respectively. Triethanolamine (TEA, SRL) was used as a simple mesoporous structure directing agent. Tetraethyl ammonium hydroxide (TEAOH, 35%, Sigma Aldrich) was used as a base. In a typical catalyst preparation 20 g of TEOS and 0.67 g of tin chloride in 2 g of water were stirred for 10 minutes. A mixture of TEA (14.3 g) and water (3 g) was then added to the above mixture and stirred vigorously for 1 h. Finally, TEAOH (13 g) was added dropwise to the previous solution under continuous stirring for another 2 h. The final gel composition was $1\text{SiO}_2 : 0.02\text{SnO}_2 : 0.3\text{TEAOH} : 1\text{TEA} : 10\text{H}_2\text{O}$. The obtained gel was aged at 30 °C for 16 h and then dried at 100 °C for 20 h. The final solid was transferred into an autoclave for hydrothermal treatment at 180 °C for 6 h and subsequently calcined at 600 °C for 10 h to remove the organic moieties.

2.2. Characterization of SnTUD-1

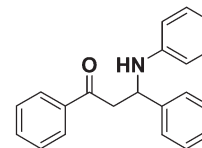
Powder X-ray diffraction (XRD) measurements were carried out on a Bruker D8 diffractometer with a nickel filtered Cu K α ($\lambda = 1.5418 \text{ \AA}$) radiation source, operating at 40 kV and 40 mA. Transmission electron microscopy (TEM) was performed on FEI Tecnai G2 fitted with a CCD camera. The sample was suspended in ethanol and deposited on a copper grid prior to analysis. Scanning electron microscopy (SEM) was performed using an ESEM Quanta 200, FEI microscope with a resolution of 20 kV. The surface area, pore volume and pore size distribution were evaluated from N_2 sorption carried out at $-196 \text{ }^\circ\text{C}$ using a Quantochrome porosimeter (QuadrasorbSI). The sample was degassed at 200 °C for 3 h before the measurement. Temperature programmed desorption (NH_3 -TPD) experiments were performed under NH_3 desorption monitoring from 100 °C to 600 °C in a Micromeritics TPR/TPD 2900 instrument with a Thermal Conductivity Detector (TCD). Diffuse reflectance UV-Vis spectra were recorded in the range of 200–800 nm with Thermoscientific Evolution 600 equipment with diffuse reflectance attachments, using BaSO_4 as a reference. FTIR spectra of KBr-diluted pellets of the sample were recorded on a Bruker instrument at room temperature with a resolution of 4 cm^{-1} averaged over 100 scans. For pyridine FTIR analysis, the catalyst was dried at 200 °C for 2 h to remove the adsorbed species. Further, 100 mg of the oven dried sample was wetted with pyridine and equilibrated for 5 h. The sample was then heated at 120 °C for 1 h at

atmospheric pressure to remove the physisorbed pyridine and FTIR analysis was carried out in the DRIFT mode. X-ray photoelectron spectroscopy (XPS) measurements were performed in an ultra-high vacuum (UHV) multipurpose surface analysis system (SpecsTM model, Germany) using a conventional X-ray source (XR-50, Specs, Mg-K α , 1253.6 eV) in a “stop-and-go” mode. The survey and detailed O, Si and Sn were recorded at room temperature with a Phoibos 150-MCD energy analyzer. The sample was deposited on a sample holder using double-sided adhesive tape and afterwards evacuated under vacuum ($<10^{-6}$ Torr) overnight. The binding energies were referenced to the C1s line at 284.6 eV from adventitious carbon. The ^{29}Si MAS NMR spectra (pulse: 6 μs ; recycle delay: 600 s) were recorded on a Bruker ACP-400 multinuclear spectrometer at 79.45 MHz. The chemical shifts have been referenced to tetramethylsilane (TMS) as an external standard.

ICP-OES leaching studies were conducted on a Perkin-Elmer Optima 5300 DV instrument. Samples (the catalyst, the filtrate after first use and subsequent filtrates and recovered catalysts, 10 mg each) were digested in 0.5 mL HF and then completed with 25 mL distilled water prior to analysis. A wavelength of 189.927 nm for Sn was used in the analysis.

2.3. Catalytic application of SnTUD-1 for Mannich-type reactions

The Mannich-type reaction was carried out at room temperature in a 10 mL closed reaction tube. SnTUD-1 catalyst (100 mg) was added to a solution containing a mixture of aldehyde (1 mmol), ketone (1 mmol) and amine (1 mmol) in ethanol (5 mL) solvent. The progress of the reaction is monitored using TLC. The reaction mixture was stirred at 750 rpm for an appropriate time and then filtered. The filtrate was washed with a sodium bicarbonate (NaHCO_3) solution followed by distilled water and dried over sodium sulphate (Na_2SO_4). The final organic layer was evaporated and the crude product was purified by silica gel column chromatography with petroleum ether–ethyl acetate (5:1). The structures of products were confirmed by ^1H NMR and FTIR in comparison with the literature. Examples of product characterisation are shown below:



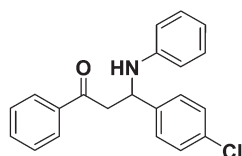
1,3-diphenyl-3-(phenylamino)propan-1-one

(Table 1, entry 1) A white solid, ^1H NMR (500 MHz, CDCl_3): δ 3.56–3.43 (m, 2H), 5.03 (m, 1H), 6.62–6.57 (d, 2H), 6.81–6.66 (m, 1H), 7.08–7.15 (m, 2H), 7.22–7.34 (m, 4H), 7.55–7.58 (m, 2H), 7.89–7.93 (m, 2H); ^{13}C NMR (500 MHz, CDCl_3): 46.4, 54.9, 59.6, 118.0, 127.5, 128.3, 128.9, 133.5, 136.8, 147.0, 198.4; FTIR (KBr, cm^{-1}): 3380, 3059, 3021, 2921, 1671, 1596, 1500, 1218, 1180, 748.

Table 1 Mannich-type three component couplings catalysed by SnTUD-1^a

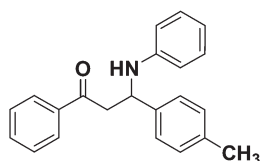
Entry	Aldehyde R ₁	Ketone R ₂	Amine R ₃	<i>t</i> (h)	Yield ^b
Blank	H	H	H	12	— ^c
1	H	H	H	12	89
2	4-Cl	H	H	10	80
3	4-CH ₃	H	H	10	82
4	4-C ₂ H ₅	H	H	12	75
5	4-OCH ₃	H	H	12	65
6	2-NO ₂	H	H	24	—
7	4-Br	H	H	10	80
8	H	Cyclohexanone	H	24	60
9	H	4'-Methyl acetophenone	H	24	—
10	H	4-Cl	H	12	70
11	H	Acetone	H	6	40
12	H	H	4-Cl	12	73

^a Reaction conditions: benzaldehyde (1 mmol), acetophenone (1 mmol), aniline (1 mmol), ethanol (3 mL), catalyst (100 mg), room temperature. ^b Isolated yield, products are confirmed by ¹H NMR and FTIR. ^c Reaction carried out with purely siliceous TUD-1 as a catalyst.

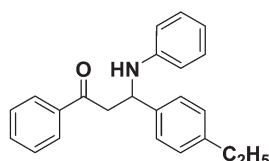


3-(4-chlorophenyl)-1-phenyl-3-(phenylamino)propan-1-one

(Table 1, entry 2) A white solid, ¹H NMR (500 MHz, CDCl₃): δ 3.58 (br, 2H), 5.01 (t, 1H), 6.66 (d, *J* = 8.1 Hz, 2H), 6.78 (m, 1H), 6.87–6.97 (b, 2H), 7.15 (t, *J* = 7.5 Hz, 2H), 7.32–7.22 (m, 1H), 7.40–7.35 (m, 2H), 7.56–7.52 (m, 1H), 7.88 (d, *J* = 7.2 Hz, 2H); FTIR (KBr, cm⁻¹): 3392, 3047, 2921, 1664, 1602, 1501, 1287, 1093, 754.

1-phenyl-3-(phenylamino)-3-*p*-tolylpropan-1-one

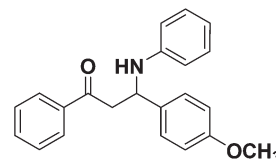
(Table 1, entry 3) A white solid, ¹H NMR (500 MHz, CDCl₃): δ 2.4 (s, 3H), 3.50–3.40 (m, 2H), 4.98 (t, 1H), 6.25 (d, *J* = 7.9 Hz, 2H), 6.90 (br, 1H), 7.1–7.0 (m, 2H), 7.18 (d, 2H), 7.26 (d, 2H), 7.43–7.33 (m, 2H), 7.55–7.46 (m, 1H), 7.92 (d, 2H); FTIR (KBr, cm⁻¹): 3388, 3037, 2923, 1668, 1603, 1505, 1287, 993, 752.



3-(4-Ethylphenyl)-1-phenyl-3-(phenylamino)propan-1-one

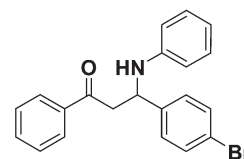
(Table 1, entry 4) A white solid, ¹H NMR (500 MHz, CDCl₃): δ 1.3–1.2 (t, *J* = 7 Hz, 3H), 2.72 (m, 2H), 3.49–3.40 (m, 2H), 4.99 (t, 1H), 6.25 (d, *J* = 7.9 Hz, 2H), 6.78 (m, 1H), 7.2–7.1 (m, 2H),

7.29 (m, 2H), 7.46–7.36 (d, 2H), 7.56–7.46 (m, 1H); FTIR (KBr, cm⁻¹): 3380, 3030, 2932, 1669, 1597, 1507, 1281, 1107, 842, 740, 687, 551.



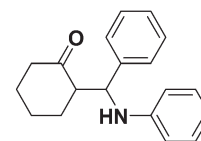
3-(4-methoxyphenyl)-1-phenyl-3-(phenylamino)propan-1-one

(Table 1, entry 5) A pale yellow solid, ¹H NMR (500 MHz, CDCl₃): δ 3.47–3.41 (b, 2H), 3.79 (s, 3H), 5.01 (t, 1H), 6.49 (d, *J* = 8.1 Hz, 2H), 6.63 (d, 1H), 6.90–6.86 (m, 2H), 7.26 (d, *J* = 8.0 Hz, 2H), 7.43 (m, 2H), 7.56–7.52 (m, 1H), 7.89 (d, 2H); FTIR (KBr, cm⁻¹): 3396, 3042, 2924, 1662, 1596, 1501, 1282, 752.



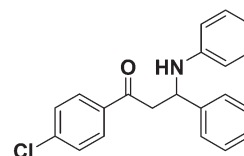
3-(4-bromophenyl)-1-phenyl-3-(phenylamino)propan-1-one

(Table 1, entry 7) A yellowish solid, ¹H NMR (500 MHz, CDCl₃): δ 3.58 (br, 2H), 4.99 (t, 1H), 6.50 (d, *J* = 8.4 Hz, 2H), 6.65 (m, 1H), 6.89–6.96 (m, 2H), 7.15 (t, 2H), 7.32–7.22 (m, 1H), 7.40–7.35 (m, 2H), 7.50–7.46 (m, 1H), 7.56–7.52 (m, 2H); FTIR (KBr, cm⁻¹): 3390, 3047, 1665, 1600, 1280, 1092, 756, 684.



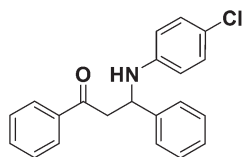
2-(phenyl (phenylamino) methyl) cyclohexanone

(Table 1, entry 8) A white solid, ¹H NMR (500 MHz, CDCl₃): δ 1.80–1.62 (m, 3H), 1.98 (m, 3H), 2.44–2.30 (m, 2H), 2.80–2.74 (m, 1H), 4.62 (d, *J* = 7.4 Hz, 0.99H), 4.81–4.78 (d, 0.16H), 6.56–6.54 (d, 2H), 6.65–6.62 (t, 1H), 7.05–7.01 (t, *J* = 8.0 Hz, 2H), 7.24–7.20 (t, 1H), 7.34–7.30 (m, 2H), 7.58 (d, 2H), 8.16 (d, 2H); FTIR (KBr, cm⁻¹): 3391, 1689, 1088, 762.



1-(4-chlorophenyl)-3-phenyl-3-(phenylamino)propan-1-one

(Table 1, entry 10) A white solid, ¹H NMR (500 MHz, CDCl₃): δ 3.42 (m, 2H), 5.1 (s, 1H), 6.25 (d, *J* = 7.9 Hz, 2H), 6.78 (m, 1H), 7.2–7.1 (m, 2H), 7.29 (m, 2H), 7.46–7.36 (d, 2H), 7.56–7.46 (m, 1H), 7.82 (d, 2H); FTIR (KBr, cm⁻¹): 3386, 3045, 2921, 1668, 1604, 1501, 1289, 759, 619.



3-(4-chlorophenylamino)-1,3-diphenylpropan-1-one

(Table 1, entry 12) A pale yellow solid, ^1H NMR (500 MHz, CDCl_3): δ 3.42 (m, 2H), 5.01 (t, 1H), 6.42 (m, 2H), 6.86 (d, J = 8.1 Hz, 2H), 7.14–7.10 (m, 2H), 7.25 (t, 2H), 7.34–7.29 (m, 2H), 7.42 (m, 2H), 7.86 (d, 2H); FTIR (KBr, cm^{-1}): 3380, 2921, 1670, 1599, 1279, 1085, 756, 616.

3. Results and discussion

A broad peak with low intensity approximately at $2\theta = 0.5^\circ$ was observed to be present in small angle XRD patterns (Fig. 1a), typical of disordered mesoporous materials such as TUD-1.^{24,42} Despite the amorphous silica peak around 2θ of $15\text{--}30^\circ$ observed in high angle powder XRD measurements (Fig. 1b), the presence of a diffraction line corresponding to tetragonal SnO_2 nanoparticles (rutile structure) was evidenced from indexed peaks at 2θ (27 , 34 and 52°), in good agreement with literature reports.^{16,21} Using the Debye–Sherrer equation, the average crystalline size of SnO_2 particles of SnTUD-1 was calculated to be *ca.* 20 nm.

N_2 sorption isotherms of SnTUD-1 (Fig. 2a) displayed a Type IV isotherm with a hysteresis loop, typical of TUD-1 type materials.²⁴ SnTUD-1 exhibited an average adsorption pore size distribution of 7.4 nm (Fig. 2b) and a BET surface area and pore volume of $555\text{ m}^2\text{ g}^{-1}$ and $1.02\text{ cm}^3\text{ g}^{-1}$, respectively.

Diffuse reflectance UV-Vis spectra of SnTUD-1 (Fig. 3a) showed two main absorption bands centered at *ca.* 220 and 280 nm which can be assigned to the presence of isolated four co-ordinated Sn^{4+} ions^{18,22} and hexacoordinated polymeric Sn–O–Sn type species.^{12,14} These findings support the presence of both framework incorporated tin and extraframework SnO_2

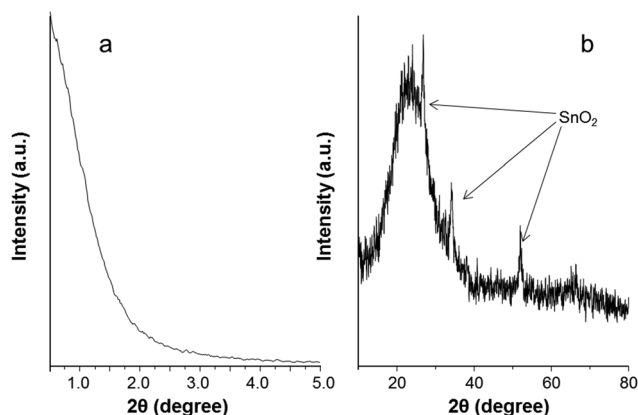


Fig. 1 Powder XRD pattern of SnTUD-1 in (a) low angle and (b) high angle.

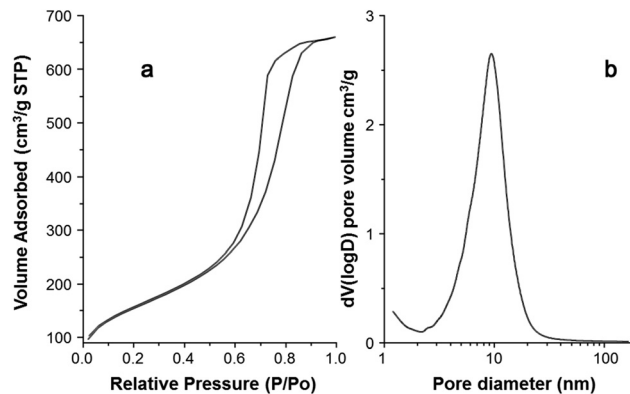


Fig. 2 Nitrogen sorption isotherm (a) and adsorption pore size distribution (b) of SnTUD-1.

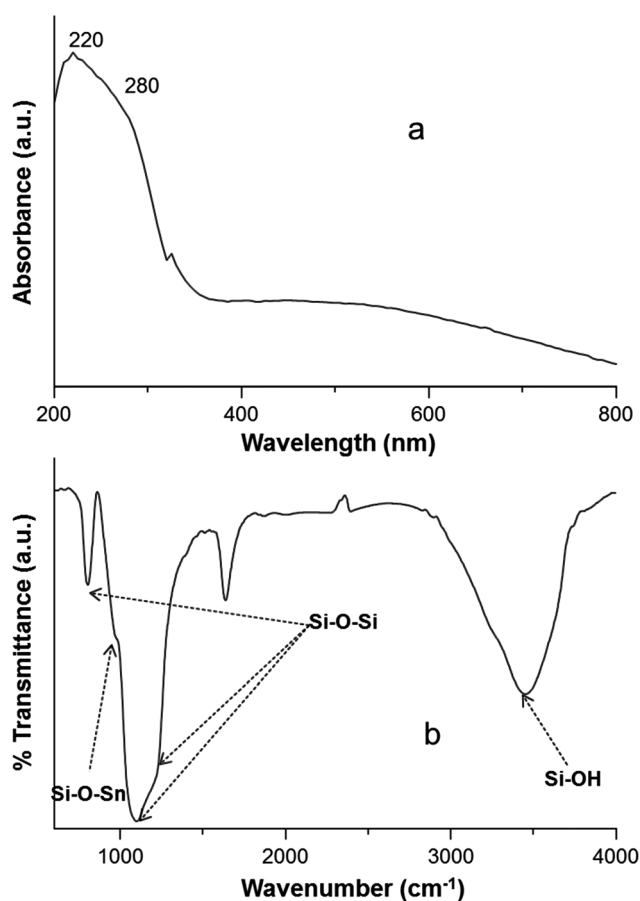


Fig. 3 Diffuse reflectance UV-Vis (a) and FTIR (b) spectra of SnTUD-1.

species, in good agreement with the XRD results. FTIR spectra of the calcined SnTUD-1 displayed a broad peak at 3480 cm^{-1} attributed to the O–H stretching vibration of surface Si–OH groups as well as residual water present in the materials (Fig. 3b). Bands at 1230 , 1080 and 798 cm^{-1} could also be assigned to symmetric and asymmetric stretching of $\equiv\text{Si-O-Si}\equiv$ vibrations, while the weak band at 960 cm^{-1} can be attributed to Si–O–Sn linkages, as previously reported,^{12,18} which

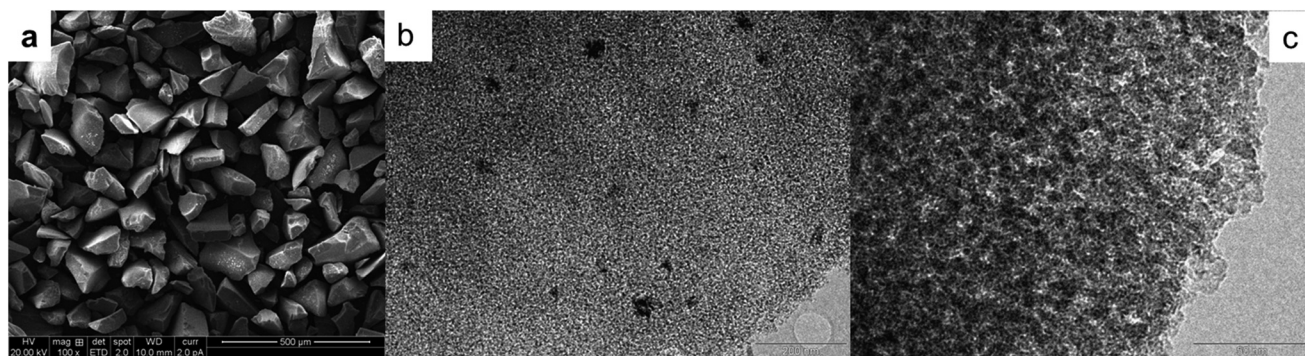


Fig. 4 SEM (a) and TEM (b and c) images of SnTUD-1.

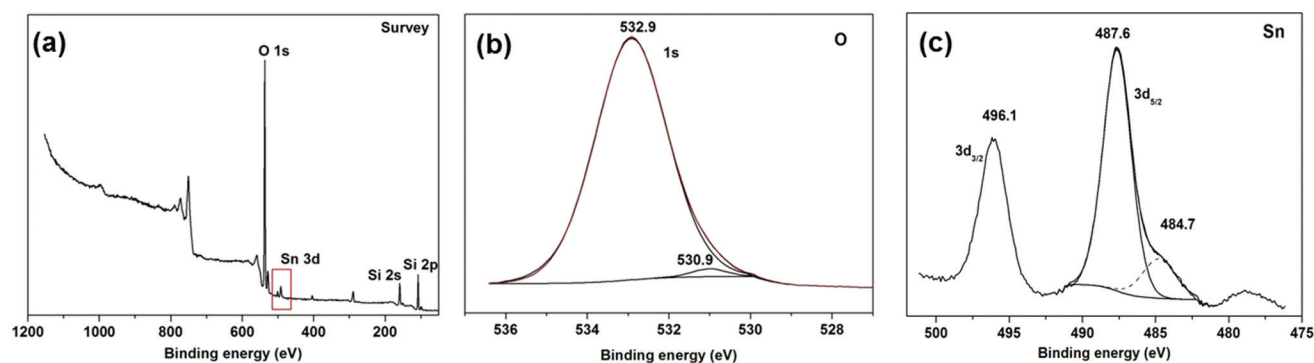


Fig. 5 XPS spectrum of SnTUD-1: (a) survey, (b) O1s, and (c) Sn3d.

again confirmed the partial incorporation of Sn into the framework of TUD-1.

SEM micrographs of Sn-TUD-1 samples depicted micrometer sized ($\sim 50 \mu\text{m}$) irregular and agglomerated stone-like particles (Fig. 4a). The disordered wormhole type morphology of TUD-1 was also evidenced from TEM micrographs (Fig. 4b and c). Tin oxide nanoparticles (which appeared as dark spots, Fig. 4b) were found to be present mostly as agglomerates at the surface of TUD-1, with nanoparticle sizes 20–30 nm. These findings are in good agreement with XRD observations. Interestingly, a number of highly dispersed tin oxide nanoparticles (*ca.* 6 nm) were also present in the materials as can be seen in Fig. 4. SEM and TEM-EDAX spectra (ESI, S1 and S2†) showed the presence of Si, O, and Sn. The average amount of Sn atoms present in the TUD-1 silica matrix was estimated to be about 2 wt% (atomic) from TEM-EDAX and SEM-EDAX, in good correlation with the theoretical $\text{SiO}_2/\text{SnO}_2$ molar ratio in the synthesis gel.

A typical XPS spectrum of the SnTUD-1 sample is shown in Fig. 5. The survey scan (Fig. 5a) of SnTUD-1 showed peaks mainly around 104, 155, 499 and 535 eV that are assigned to Si2p, Si2s, Sn3d and O1s, respectively. The core level O1s spectrum (Fig. 5b) of SnTUD-1 showed an asymmetric signal, which can be deconvoluted into two peaks. The main peak at 532.9 eV can be correlated to Si–O bonds from silica (SiO_2) as compared to the low intense peak (*ca.* 530.9 eV) which is believed to arise from the O1s contribution of tin oxides

(SnO_x). This observation further confirms the presence of tin oxide nanoparticles as observed from XRD, DRS-UV-Vis and TEM studies. However, Sn3d XPS spectra (Fig. 5c) of SnTUD-1 provided the most interesting findings with two clearly distinguished tin oxide (SnO_x) components in Sn3d_{5/2} (Fig. 5c). A distinction between Sn(IV) oxide and Sn(II) oxide is not possible by XPS as only Mössbauer spectroscopy will be able to provide insightful differentiation between Sn(IV) and lower-valency tin species.^{43,44} In any case, the major contribution with a large area (*ca.* 487.6 eV) is, in principle, likely to be related to framework Sn(IV) species in the materials in which Sn^{4+} replaced Si^{4+} atoms. However, the presence of other tin oxide species as part of this major contribution cannot be ruled out based only on XPS studies. Comparatively, the minor contribution at lower binding energy (*ca.* 484.7 eV), which is very close to the binding energy of Sn^0 (*ca.* 484 eV),⁴⁴ indicates the presence of different tin oxide species which in principle may be mostly related to the observed tin oxide extraframework tin oxide nanoparticles which could potentially include a contribution of reduced tin oxide species in the systems as these cannot be ruled out by XPS.^{43,44}

²⁹Si MAS NMR spectra of SnTUD-1 exhibited clear peaks at -93 ppm (Q_2), -103 ppm (Q_3) and -110 (Q_4), which can be attributed to $(\text{SiO})_2\text{Si}(\text{OH})_2$, $(\text{SiO})_3\text{SiOH}$ and $(\text{SiO})_4$ units respectively (Fig. 6). Very similar peak profiles have been previously reported in pure Si-TUD-1 materials.²³

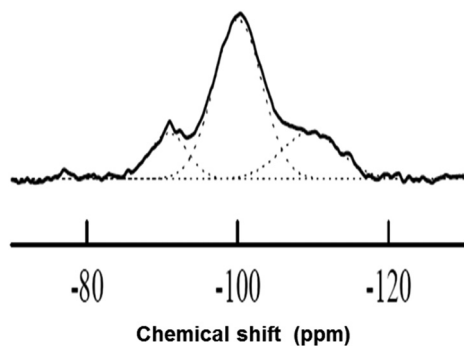
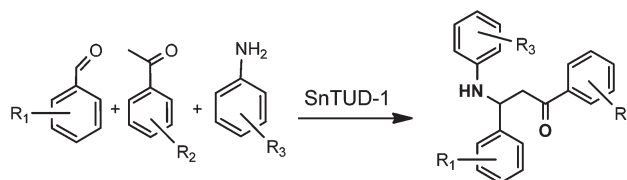


Fig. 6 ^{29}Si MAS NMR of SnTUD-1.

The surface acidity of the materials was subsequently investigated by NH_3 -TPD and DRIFT studies of adsorbed pyridine. Three major bands were observed in the FTIR spectra of adsorbed pyridine in the region of $1400\text{--}1700\text{ cm}^{-1}$ (Fig. 7a). The bands observed at 1592 and 1445 cm^{-1} can be assigned to pyridine bonded to Lewis acid sites.⁴⁵ Remarkably no appreciable contribution was observed for Brønsted acid sites (band at *ca.* $\sim 1545\text{ cm}^{-1}$),⁴⁵ which indicates the exclusive presence of Lewis acid sites in SnTUD-1 materials upon Sn incorporation. Complementary ammonia TPD results pointed out the presence of Lewis acid sites of varying strength in the material, exemplified by two distinct desorption peaks centered at $203\text{ }^\circ\text{C}$ and $480\text{ }^\circ\text{C}$ (Fig. 7b), with a total material acidity of 0.24 mmol NH_3 per g. A majority of weak to moderate strength acid sites are evidenced from the large desorption peak in the low temperature region. Interestingly, a certain contribution of strong acid sites also seems to be present in SnTUD-1 as shown by the desorption peak at a relatively high temperature region ($480\text{ }^\circ\text{C}$).

Having proved the nature and type of acid sites and tin species in the material, the activity of SnTUD-1 in the one-pot Mannich reaction of substituted aldehydes, amines and ketones was subsequently investigated (Scheme 1). A blank reaction with siliceous TUD-1 did not yield any desirable



Scheme 1 One-pot Mannich reaction of substituted aldehyde, amine and ketone catalyzed by SnTUD-1.

product. The SnTUD-1 catalysed reaction was found to proceed effectively in the following solvent order: ethanol > acetonitrile > dichloromethane > water. Upon optimisation of the systems, reactions were carried out using ethanol as a benign solvent with substituted benzaldehydes, aniline and acetophenone as model substrates. β -Amino carbonyl compounds were obtained in moderate to good yields ($60\text{--}80\%$) after 12 h at room temperature.

The scope of the reaction was further examined with various *ortho*- and *para*-substituted ketones, aldehydes and amines under similar conditions (Table 1). Remarkable yields of products ($>85\%$) were achieved using SnTUD-1 as a catalyst (Table 1, entry 1). Substituted benzaldehyde with electron withdrawing or donating groups in *para* position gave the corresponding β -amino carbonyls in good yields ($60\text{--}85\%$), whereas *ortho*-substituted benzaldehyde such as 2-nitrobenzaldehyde (Table 1, entry 7) provided no yield of the expected product due to steric effects and imine formation. Electron-deficient amines (4-chloroaniline) and ketones (4-chloroacetophenone) yielded 70% of the corresponding β -amino compounds (Table 1, entries 10 and 12). Interestingly, aliphatic ketones (*e.g.* acetone) gave poor yields (Table 1, entry 11) with an important number of unidentifiable products observed after reaction workup, indicating an unselective reaction of acetone with aniline and benzaldehyde. The reactivities of 4-methyl acetophenone and cyclohexanone were comparably lower than that of acetophenone; only trace amounts of products were obtained for $-\text{CH}_3$ substituted acetophenone (Table 1, entries

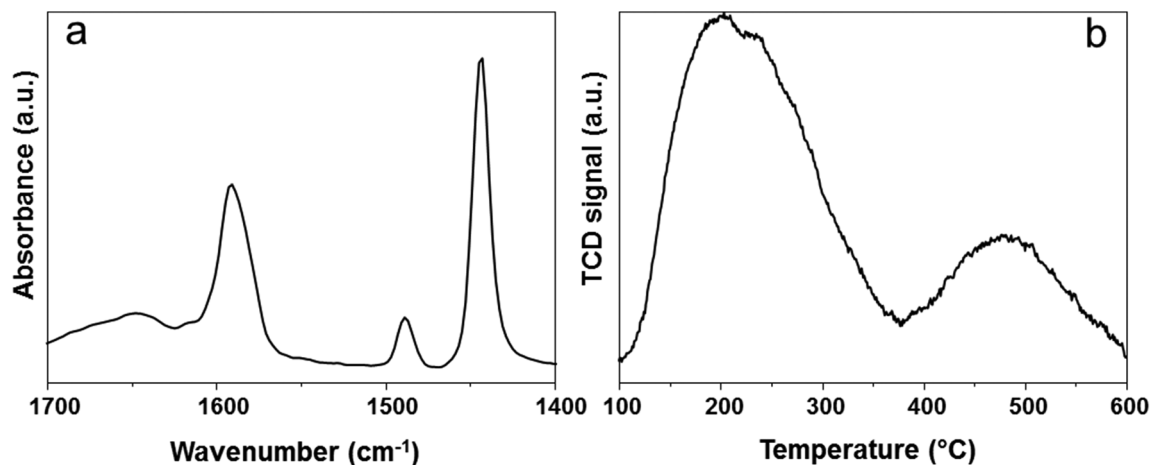
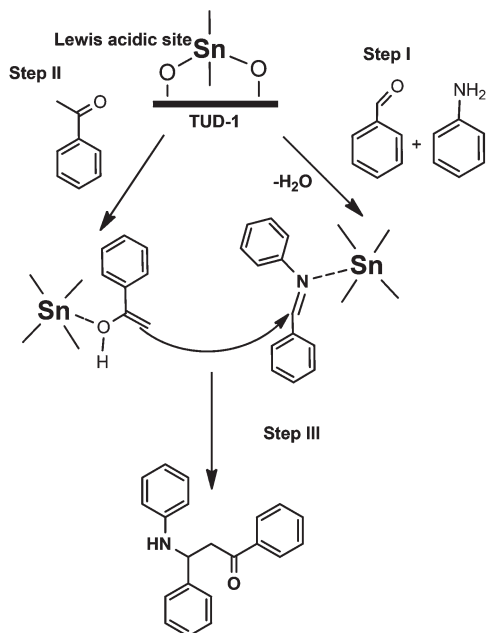


Fig. 7 NH_3 -TPD profile (a) and FTIR spectra of adsorbed pyridine (b) of SnTUD-1.



Scheme 2 Proposed reaction pathway for Mannich reaction catalyzed by SnTUD-1.

8 and 9). Apart from the desired product, nearly 10–20% formation of the corresponding imines (Schiff base; their formation was observed within 1 h of reaction) was noticed in the investigated reactions which did not react further to yield the Mannich product even after 48 h.

Since the Schiff base formation was observed within 1 h of reaction, a plausible mechanistic pathway proposed here is the formation of an iminium ion from aldehydes and amines (Scheme 2, step 1). The formation of an enol takes place in a subsequently slow expected step (Scheme 2, step 2) to then lead to β -amino carbonyl compounds. This step can be accelerated on the coordinatively available Lewis acidic sites of SnTUD-1.^{41,46} After reaction, SnTUD-1 was filtered, and reused for up to four cycles (Fig. 8). The material was found to preserve over 90% of its initial activity after 4 cycles, indicating the stability of the catalyst under the investigated reaction conditions. Studies on Sn leaching under the investigated reaction conditions were subsequently conducted to ascertain the heterogeneous nature of the protocol. For this purpose, the catalyst was filtered off half-way through the reaction (after 6 h) and the filtrate with potentially Sn leached species was left to react for a longer period of time (12 h). The filtrate was also analyzed by ICP-OES for Sn content. In parallel, the recovered catalyst from the reaction was washed thoroughly and conditioned in ethanol and water prior to another reaction run with fresh reagents. Results from the filtrate continued reaction in the first run indicated that the reaction proceeded somehow in the absence of catalyst due to Sn leaching. ICP-OES results confirmed significant Sn leaching into solution (*ca.* 0.71 wt%, 0.14 mg L⁻¹ Sn), accounting for over a third of the total Sn content in SnTUD-1. However, only the formation of the iminium ion (from aldehyde and amine) was

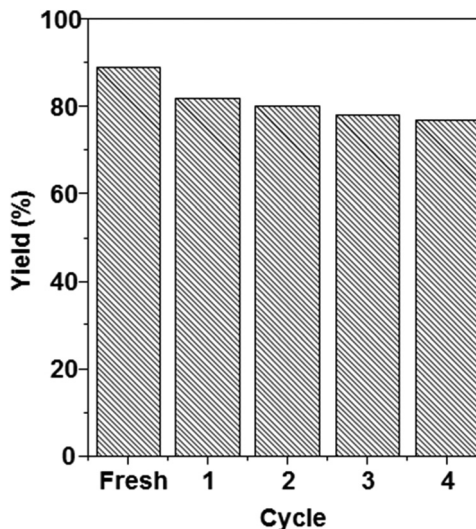


Fig. 8 Reusability cycles of SnTUD-1 for benzaldehyde, acetophenone and aniline coupling reactions.

gratifyingly observed without any subsequent formation of the desired Mannich product. Comparatively, the reaction with the recovered SnTUD-1 containing a reduced *ca.* 1.3 wt% Sn (after leaching) progressed under typical reported yields at room temperature (>80%, 12 h reaction, similar to that of cycle 1 in Fig. 8). These findings pointed out the need for Lewis acidic Sn framework species in SnTUD-1 to specifically promote step 2 (Scheme 2) leading to the final β -amino carbonyl compounds, in good agreement with our proposed mechanism. Importantly, ICP-OES analysis of the filtrate from subsequent reuses of the catalyst (cycles 2, 3 and 4, Fig. 8) showed no leaching of Sn species into solution, indicating the high stability of SnTUD-1 after the first use under the investigated reaction conditions. The catalyst was stable and highly active upon reuse. Results also confirmed the truly heterogeneous nature of the reaction and pointed out the presence of weakly incorporated Sn species on SnTUD-1 which could have been simply removed prior to the first run by a thorough conditioning step under ethanol reflux.

Further studies are currently ongoing to expand the application of SnTUD-1 in related acid-catalysed chemistries including alkylations and acylations as well as biomass-related valorisation processes (*e.g.* isomerisations of sugars).

4. Conclusions

A novel Sn-incorporated TUD-1 material has been successfully synthesised by a direct hydrothermal method using inexpensive TEA as a structure directing agent. UV-Vis, FTIR and XPS confirmed the presence of framework Sn⁴⁺ in tetrahedral coordination in SnTUD-1, with the presence of tin oxide nanoparticles on the surface as evidenced from UV-Vis, XRD and TEM. SnTUD-1 featured a high surface area and an interesting Lewis acidity, with acid sites of varying strength from Sn

incorporation, which conferred excellent activities on Mannich-type three component coupling reactions at room temperature. A range of β -aminocarbonyl compounds could be synthesized in moderate to very good yields under very mild reaction conditions. The proposed Lewis-acidic material is envisaged to have multiple applications in acid catalysed processes including biomass valorisation chemistries currently under investigation in our laboratories.

Acknowledgements

The authors are thankful to Prof. B. Viswanathan, NCCR, IIT-Madras for providing laboratory facilities to carry out this work. M.P.P. is thankful to DST-FIST and UGC – Research Fellowship scheme. R.L. gratefully acknowledges Ministerio de Ciencia e Innovacion, Gobierno de España for the concession of a Ramon y Cajal contract (ref. RYC-2009-04199) and Consejería de Ciencia e Innovacion, Junta de Andalucía for funding under the project P10-FQM-6711. Funding from projects CTQ-2010-18126 (MICINN) and P09-FQM-4781 (Consejería de Ciencia e Innovacion, Junta de Andalucía) is also gratefully acknowledged. Revisions suggested by reviewers along the lines of Sn leaching and stability studies are kindly acknowledged and deeply appreciated.

References

- 1 K. Tanabe and W. F. Hölderich, *Appl. Catal., A*, 1999, **181**, 399–434.
- 2 K. Wilson and J. H. Clark, *Pure Appl. Chem.*, 2000, **72**, 1313–1319.
- 3 A. Taguchi and F. Schuth, *Microporous Mesoporous Mater.*, 2005, **77**, 1–45.
- 4 A. Corma, L. T. Nemeth, M. Renz and S. Valencia, *Nature*, 2001, **412**, 423–425.
- 5 M. Renz, T. Blasco, A. Corma, V. Fornes, R. Jensen and L. Nemeth, *Chem.–Eur. J.*, 2002, **8**, 4708–4717.
- 6 A. Corma, M. E. Domine and S. Valencia, *J. Catal.*, 2003, **215**, 294–304.
- 7 M. Boronat, P. Concepcion, A. Corma, M. Renz and S. Valencia, *J. Catal.*, 2005, **234**, 111–118.
- 8 M. Boronat, A. Corma, M. Renz, G. Sastre and P. M. Viruela, *Chem.–Eur. J.*, 2005, **11**, 6905–6915.
- 9 M. Boronat, P. Concepcion, A. Corma and M. Renz, *Catal. Today*, 2007, **121**, 39–44.
- 10 A. Corma and M. Renz, *Angew. Chem., Int. Ed.*, 2007, **46**, 298–300.
- 11 E. A. Alarcón, L. Correa, C. Montes and A. L. Villa, *Microporous Mesoporous Mater.*, 2010, **136**, 59–67.
- 12 K. Chaudhari, T. K. Das, P. R. Rajmohanan, K. Lazar, S. Sivasanker and A. J. Chandwadkar, *J. Catal.*, 1999, **183**, 281–291.
- 13 A. Corma, M. T. Navarro and M. Renz, *J. Catal.*, 2003, **219**, 242–246.
- 14 T. R. Gaydhankar, P. N. Joshi, P. Kalita and R. Kumar, *J. Mol. Catal. A: Chem.*, 2007, **265**, 306–315.
- 15 U. S. Taralkar, P. Kalita, R. Kumar and P. N. Joshi, *Appl. Catal., A*, 2009, **358**, 88–94.
- 16 P. Shah, A. V. Ramaswamy, K. Lazar and V. Ramaswamy, *Microporous Mesoporous Mater.*, 2007, **100**, 210–226.
- 17 S. Y. Chen, H. D. Tsai, W. T. Chuang, J. J. Lee, C. Y. Tang, C. Y. Lin and S. F. Cheng, *J. Phys. Chem. C*, 2009, **113**, 15226–15238.
- 18 M. Sasidharan, Y. Kiyozumi, N. K. Mal, M. Paul, P. R. Rajamohanan and A. Bhaumik, *Microporous Mesoporous Mater.*, 2009, **126**, 234–244.
- 19 J. S. Lee, G. B. Han and M. Kang, *Energy*, 2012, **44**, 248–256.
- 20 T. M. AbdelFattah and T. J. Pinnavaia, *Chem. Commun.*, 1996, 665–666.
- 21 K. Bachari and O. Cherifi, *Appl. Catal., A*, 2007, **319**, 259–266.
- 22 S. Sisodiya, S. Shylesh and A. P. Singh, *Catal. Commun.*, 2011, **12**, 629–633.
- 23 J. C. Jansen, Z. Shan, L. Marchese, W. Zhou, N. von der Puil and T. Maschmeyer, *Chem. Commun.*, 2001, 713–714.
- 24 S. Telalovic, A. Ramanathan, G. Mul and U. Hanefeld, *J. Mater. Chem.*, 2010, **20**, 642–658.
- 25 M. J. Climent, A. Corma and S. Iborra, *Chem. Rev.*, 2011, **111**, 1072–1133.
- 26 M. J. Climent, A. Corma and S. Iborra, *RSC Adv.*, 2012, **2**, 16–58.
- 27 R. Muller, H. Goesmann and H. Waldmann, *Angew. Chem., Int. Ed.*, 1999, **38**, 184–187.
- 28 N. S. Joshi, L. R. Whitaker and M. B. Francis, *J. Am. Chem. Soc.*, 2004, **126**, 15942–15943.
- 29 A. Cordova, *Acc. Chem. Res.*, 2004, **37**, 102–112.
- 30 T. Ollevier, E. Nadeau and A. A. Guay-Begin, *Tetrahedron Lett.*, 2006, **47**, 8351–8354.
- 31 B. M. Reddy, M. K. Patil and B. T. Reddy, *Catal. Lett.*, 2008, **125**, 97–103.
- 32 R. Wang, B.-G. Li, T.-K. Huang, L. Shi and X.-X. Lu, *Tetrahedron Lett.*, 2007, **48**, 2071–2073.
- 33 M. A. Bigdeli, F. Nematy and G. H. Mahdavinia, *Tetrahedron Lett.*, 2007, **48**, 6801–6804.
- 34 P. Goswami and B. Das, *Tetrahedron Lett.*, 2009, **50**, 2384–2388.
- 35 W. Shen, L.-M. Wang and H. Tian, *J. Fluorine Chem.*, 2008, **129**, 267–273.
- 36 Y. Suling, L. Gang and L. Yunling, *Kinet. Catal.*, 2012, **53**, 689–693.
- 37 Z. Li, X. Ma, J. Liu, X. Feng, G. Tian and A. Zhu, *J. Mol. Catal. A: Chem.*, 2007, **272**, 132–135.
- 38 N. Azizi, L. Torkiyan and M. R. Saidi, *Org. Lett.*, 2006, **8**, 2079–2082.
- 39 T.-P. Loh, S. B. Liung, K.-L. Tan and L.-L. Wei, *Tetrahedron*, 2000, **56**, 3227–3237.
- 40 M. Kidwai, N. K. Mishra, V. Bansal, A. Kumar and S. Mozumdar, *Tetrahedron Lett.*, 2009, **50**, 1355–1358.
- 41 R. K. Sharma, D. Rawat and G. Gaba, *Catal. Commun.*, 2012, **19**, 31–36.

- 42 R. Maheswari, M. P. Pachamuthu and R. Anand, *J. Porous Mater.*, 2011, **19**, 103–110.
- 43 P. Biloen, J. N. Helle, H. Verbeek, F. M. Dautzenberg and W. M. H. Sachtler, *J. Catal.*, 1980, **63**, 112–118.
- 44 S. D. Gardner, G. B. Hoflund and D. R. Schryer, *J. Catal.*, 1989, **119**, 179–186.
- 45 J. M. Campelo, D. Luna, R. Luque, J. M. Marinas, A. A. Romero, J. J. Calvino and M. P. Rodriguez-Luque, *J. Catal.*, 2005, **230**, 327–338.
- 46 S. S. Mansoor, K. Aswin, K. Logaiya and S. P. N. Sudhan, *J. Saudi Chem. Soc.*, 2012, DOI: 10.1016/j.jscs.2012.04.008.